

See discussions, stats, and author profiles for this publication at: <https://www.researchgate.net/publication/370266616>

# Effects of the additions of fin and suction on aerodynamic drags of vehicle model

Conference Paper · April 2023

DOI: 10.1063/5.0126979

CITATIONS

0

READS

21

5 authors, including:



**Rustan Tarakka**

Universitas Hasanuddin

39 PUBLICATIONS 119 CITATIONS

[SEE PROFILE](#)



**Nasaruddin Salam**

Universitas Hasanuddin

31 PUBLICATIONS 139 CITATIONS

[SEE PROFILE](#)



**Jalaluddin Jalaluddin**

Universitas Hasanuddin

40 PUBLICATIONS 365 CITATIONS

[SEE PROFILE](#)



**Muhammad Ihsan Mukrim**

LLDIKTI IX Sulawesi

50 PUBLICATIONS 82 CITATIONS

[SEE PROFILE](#)

Some of the authors of this publication are also working on these related projects:



Kajian Kinerja Jalan Kabupaten Pinrang [View project](#)



Beton Menggunakan Agregat Limbah Plastik (LIPSTIK) - BETON LIPSTIK [View project](#)

RESEARCH ARTICLE | APRIL 25 2023

## Effects of the additions of fin and suction on aerodynamic drags of vehicle model

Rustan Tarakka ✉; Jalaluddin; Nasaruddin Salam; ... et. al



AIP Conference Proceedings 2630, 020020 (2023)

<https://doi.org/10.1063/5.0126979>



CrossMark

### Articles You May Be Interested In

Analysis of the effect of rear-window tilt on aerodynamic drags of sedan vehicle model

*AIP Conference Proceedings* (April 2023)

Effects of the application of inlet disturbance bodies to drag coefficients of tandem arranged square cylinders

*AIP Conference Proceedings* (November 2022)

Numerical investigation on the effect of rear wing on aerodynamic performance of race car

*AIP Conference Proceedings* (November 2022)

Time to get excited.  
Lock-in Amplifiers – from DC to 8.5 GHz

[Find out more](#)

# Effects of The Additions of Fin and Suction on Aerodynamic Drags of Vehicle Model

Rustan Tarakka<sup>1, a)</sup>, Jalaluddin<sup>1, b)</sup>, Nasaruddin Salam<sup>1, c)</sup>, Muhsyafir<sup>1, d)</sup>  
Muhammad Ihsan Mukrim<sup>2, e)</sup>

<sup>1</sup> Department of Mechanical Engineering, Hasanuddin University, Gowa. South Sulawesi, Indonesia

<sup>2</sup> Sekolah Tinggi Teknik Baramuli, Pinrang. South Sulawesi, Indonesia

a) corresponding authors rustan\_tarakka@yahoo.com

b) jalaluddin\_had@yahoo.com,

c) nassalam.unhas@yahoo.co.id,

d) muhsyafir234@gmail.com

e) muhammadihsan@alumni.ait.asia

**Abstract.** The aerodynamic aspect of a vehicle is related to the emergence of drag on the vehicle. Aerodynamic drag arises due to the low pressure and flow separation that occurs at the rear of the car. This affects the amount of fuel consumption used by vehicles. The earlier the emergence of the flow separation, the larger the wake area will be and cause a decrease in pressure at the rear of vehicles. Therefore, efforts are needed to reduce the aerodynamic drag on the vehicle so that it can delay the flow separation and increase the pressure at the rear of the vehicle by implementing flow control. This study aims to analyze the effect of passive control in the form of fin and active control in the form of suction on the flow characteristics, pressure field, and aerodynamic drag of the vehicle model. The test model used is Ahmed's body modified in flow direction with a slant front geometry of 25°. The research was carried out with two approaches: a computational approach by using the Computational Fluid Dynamics (CFD) program ANSYS Fluent 6.3.26, and an experimental approach by using a subsonic wind tunnel. The upstream flow speed is 22.2 m/s and the suction speed is 0.5 m/s, 1.0 m/s, and 1.5 m/s. The results show that the addition of passive fin control and active suction control could delay flow separation, reduce turbulence, and increase pressure at the rear of the test model. The largest increase in the minimum pressure coefficient value is 56.66% and the largest aerodynamic drag coefficient reduction is 16.902% for the computational approach and 17.757% for the experimental approach which occurs at a suction speed of 0.5 m/s.

## INTRODUCTION

The recent progress of science and technology is very remarkable, especially in the field of transportation which is experiencing very rapid development. This can be indicated by the increasing production of cars in the world, one of which is the family van. This type has a large engine capacity but with a body shape that does not pay attention to aerodynamic aspects. To overcome the large aerodynamic drags in vehicles, one of the innovations made by car manufacturers is innovation in the design aspect of the car shape. Innovations continue to be made to develop an aerodynamic car body shape to delay flow separation and reduce energy consumption due to drag on the car body without neglecting ergonomic and aesthetic aspects. [1] [2].

In vehicles, the flow separation that occurs is very complex. Flow separation occurs throughout the exterior of the vehicle. This gives a remarkable influence on the complexity of the flow. This pressure difference causes the phenomenon of suction towards the back due to backflow that occurs at the rear of the vehicle [3]. The pressure difference between the front and the rear of the vehicle is a prominent contributor to the overall drag caused by the flow separation at the rear of vehicles [4]. The earlier the emergence of the flow separation, the greater the formations of wake and vortex at the rear of vehicles. This has an impact on reducing the speed of vehicles, creating more fuel consumption, and thus lowering the efficiency of vehicles [5].

The flow separation results in the formation of backflow around the object. Flow that moves regularly will split during separation and result in the decrease of the pressure distribution, and the occurrence of drag forces [6]. Efforts to minimize drag are a good step to reduce fuel consumption. By reducing aerodynamic drag by 15%,

the vehicle results in fuel consumption savings of 5-7% [7]. An interesting result of reducing aerodynamic drag is obtained by placing the control devices at the rear with orientation parallel to or transverse to the main flow [8].

Roumeas et al (2009), have conducted a numerical study on drag reduction by controlling flow separation at the rear of the vehicle. A series of simulations were carried out by using the Lattice Boltzmann 3D method with the k-epsilon RNG turbulence model, applied in an Ahmed model with an angle of tilt of 25° to the horizontal reference. The flow control devices were continuous suction placed on the sloping side of the rear of the fastback car. Results obtained indicated that suction controls provide a reattachment effect on the separated flow on the inclined plane wall of the Ahmed body and a drag reduction of up to 17% [9].

In addition, in 2016 research conducted by Marsaut Maurit Rumepea et al by adding fins to the ship's rudder found that the addition of 2 can reduce the drag value by 64% of the drag value without using fins and has the highest L/D ratio of 8.16 [10]. A similar study was also conducted by Yosafat Nugraha Putra et al in 2017 found that the addition of fins on the center bulb of the Catamaran was able to reduce the total drag by 20%, namely 1.65 N at high speed with Froude Number = 0.35, the number of fins added was 6, and with fin width 0.13 m [11]

One of the active control studies with suction was used to control flow separation at the back of the Ahmed body with a slope of 25°. The results obtained are a drag reduction of up to 18% for the suction speed  $V_s = 0.6$  times the free stream velocity [12]. The same study also conducted by Rustan Tarakka et al indicated that the face geometry and the use of active suction control in the reversed Ahmed model had a significant effect on the drag coefficient. The biggest reduction in drag coefficient occurs with a slope angle of 25° at the front, which is 14.09% [13]

A computational approach using CFD Fluent 6.3 is used in this research, aiming to understand the effect of the application of fin and suction to the aerodynamic drag of the vehicle model.

## RESEARCH METHODOLOGY

The model of this research is the bluff body model of the vehicle (reversed Ahmed body). Dimensions Length 174 mm, width 64.83 mm, height 48 mm, and the front tilt angle is 25° to the horizontal plane. Modifications to the Ahmed body model were made to resemble a passenger car which is in great demand in Indonesia, which tends to take the form of a family van. This study uses the fin model shown in figure 1. The use of passive control in the form of fins and suction active controls on the reversed Ahmed body is shown in figure 2. An upstream velocity of 22.2 m/s, and the suction speed of 0.5 m/s, 1.0 m/s, and 1.5 m/s, are used in this study.

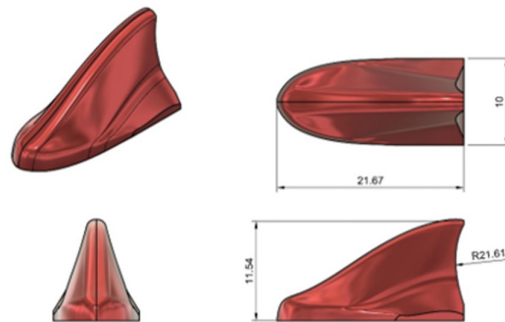


FIGURE 1. fin passive control model

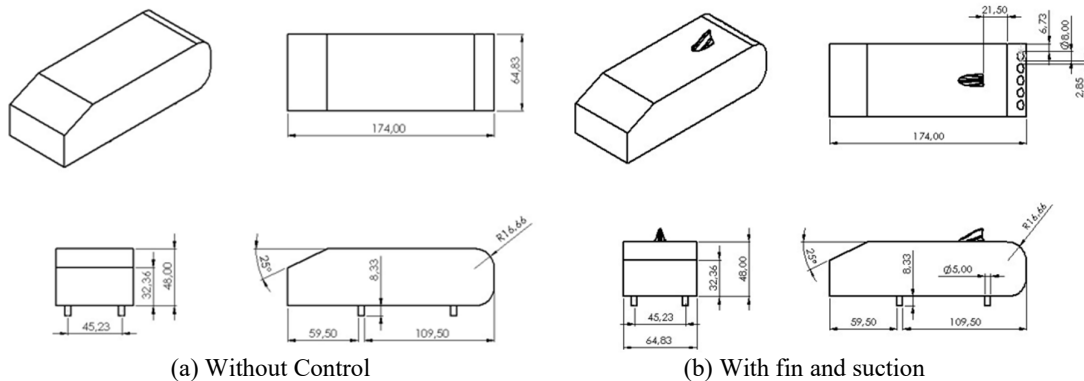


FIGURE 2. Model test of reversed Ahmed body

In this research, a computational approach was used using CFD Fluent 6.3 with a standard k-epsilon turbulence model, accommodating the equation as shown in Eq. 1 and Eq. 2.

a. Kinetic energy

$$\frac{\partial}{\partial t}(\rho k) + \frac{\partial}{\partial x_i}(\rho k u_i) = \frac{\partial}{\partial x_j} \left[ \left( \mu + \frac{\mu_t}{\sigma_k} \right) \frac{\partial k}{\partial x_j} \right] + P_k + P_b - \rho \epsilon - Y_M + S_k \quad (1)$$

b. Dissipation Rate

$$\frac{\partial}{\partial t}(\rho \epsilon) + \frac{\partial}{\partial x_i}(\rho \epsilon u_i) = \left[ \left( \mu + \frac{\mu_t}{\sigma_\epsilon} \right) \frac{\partial \epsilon}{\partial x_j} \right] + C_{1\epsilon} \frac{\epsilon}{k} (P_k + C_{3\epsilon} P_b) - C_{2\epsilon} \rho \frac{\epsilon^2}{k} + S_\epsilon \quad (2)$$

The relation between the drag force and the drag coefficient working in the vehicle model is shown in Eq. 3.

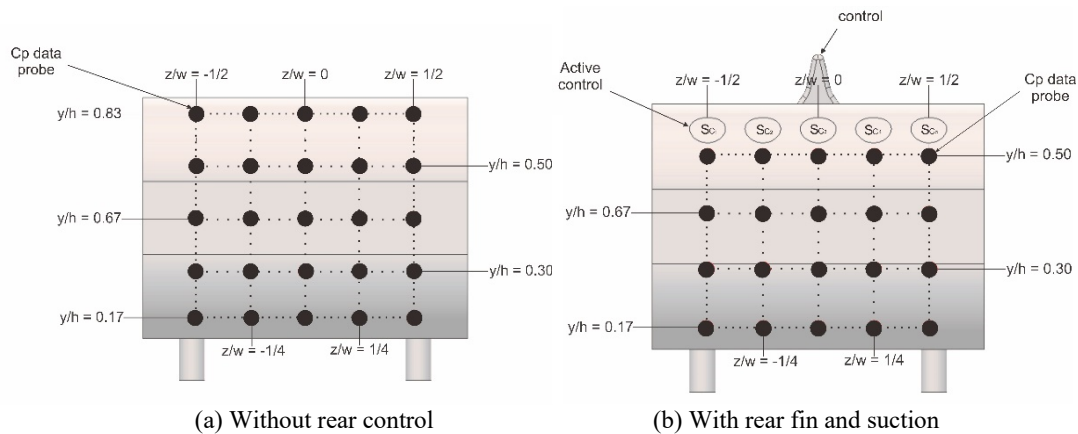
$$C_D = \frac{F}{\frac{1}{2} \rho U^2 A} \quad (3)$$

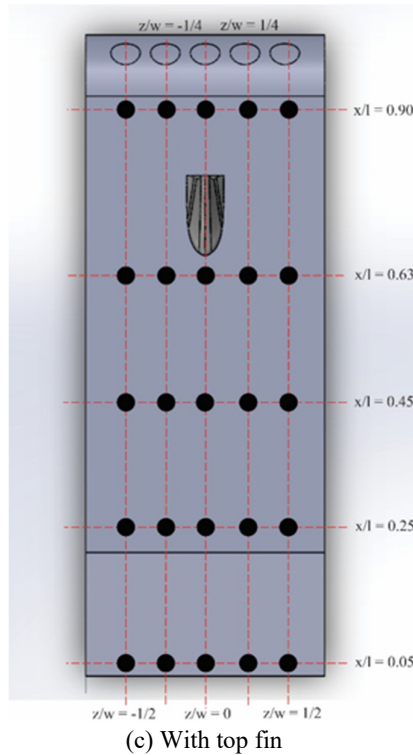
The meshing type used is tet/hybrid hex core type with boundary conditions shown in Table 1.

TABLE 1. Computational boundary condition

Boundary condition	Type	Value
Inlet	Velocity Inlet	22,2 m/s
Suction	Velocity Suction	Varied (0,5; 1,0; and 1,5 m/s)
Outlet	Pressure Outlet	0 Pa (gauge)
Model	Wall	-
Wall/Wind Tunnel	Wall	-

Pressure distribution data collection is computationally determined on the back of the vehicle model. The reason is because at that location there is a separation of flow and wake so that negative pressure appears which contributes 80% of the total drag [14]. The pressure field data collection locations were taken along the horizontal axis in five different areas on the back, designated as  $z/w = -1/2$ ,  $z/w = -1/4$ ,  $z/w = 0$ ,  $z/w = 1/2$ , and  $z/w = 1/4$ , and the five areas along the vertical axis are  $y/h = 0.83$ ,  $y/h = 0.67$ ,  $y/h = 0.50$ ,  $y/h = 0.30$ , and  $y/h = 0.17$ . Thus, 25 data points will be obtained for without control and 20 data points for models with passive control combined with active control. While at the top, five areas are taken along the vertical axis, namely  $x/L = 0.05$ ,  $x/L = 0.25$ ,  $x/L = 0.45$ ,  $x/L = 0.63$  and  $x/L = 0.9$  and five areas along the horizontal axis, namely  $z/w = -1/2$ ,  $z/w = -1/4$ ,  $z/w = 0$ ,  $z/w = 1/2$  and  $z/w = 1/4$ . The arrangement of the pressure distribution data collection are shown in figure 3.





**FIGURE 3.** Location of pressure field data ; a) without rear control, b) with rear fin and suction, and c) with top fin

## RESULTS AND DISCUSSION

### Flow characteristic

The flow characteristics of the model without control and the model with passive control and active control with an upstream speed of  $U_{sc} = 22$  m/s and each suction speed of  $U_{sc1} = 0.5$  m/s,  $U_{sc2} = 1.0$  m/s,  $U_{sc3} = 1.5$  m/s are shown in figure 4.

Figure 4 part a shows the flow separation emerging in the uncontrolled test model. The flow separation is suspected to emerge when fluid can not flow through the surface in a rather similar shape of the surface of the test model. The existence of flow separation results in backflow at the rear part of respective test models. Backflow forms due to the emergence of negative pressure, causing a backward suction phenomenon. This backward suction is the main reason for the large drag in the uncontrolled test model. In addition to that, drag is also produced by the existence of longitudinal vortex [15]. Other than that, the wake is also induced by the longitudinal vortex, formed at the rear edge of respective test models. This is due to the difference in flow velocity between the center side and the rear side of the vehicle model. The difference in velocity causes the flow from the center to move towards the side, resulting in the formation of a longitudinal vortex.

In figure 4 parts b, c and d show the flow separation that occurs in the test model using passive control and active suction control. The flow phenomenon that occurs in the addition of passive fin control and active suction control causes a reduction in the turbulence and vortex area at the rear of the vehicle compared to the test model without control. The magnitude of the reduction in the turbulent region on the back of each test model is different. This is influenced by the implementation of active suction control with varying speeds. The test model with the application of active suction control at a suction velocity of 0.5 m/s showed a smaller turbulent area and longitudinal vortex compared to the test model with the application of an active suction control at 1.0 m/s and 1.5 m/s respectively. This indicates that the effect of reducing the turbulence area and longitudinal vortex with the use of passive fin control and active suction control is more optimal in the test model with fin and suction velocity  $U_{sc} = 0.5$  m/s. The findings are in line with research by Harinaldi et al. who found that the application of active suction control at the rear of the vehicle model was able to reduce wake formation [16].

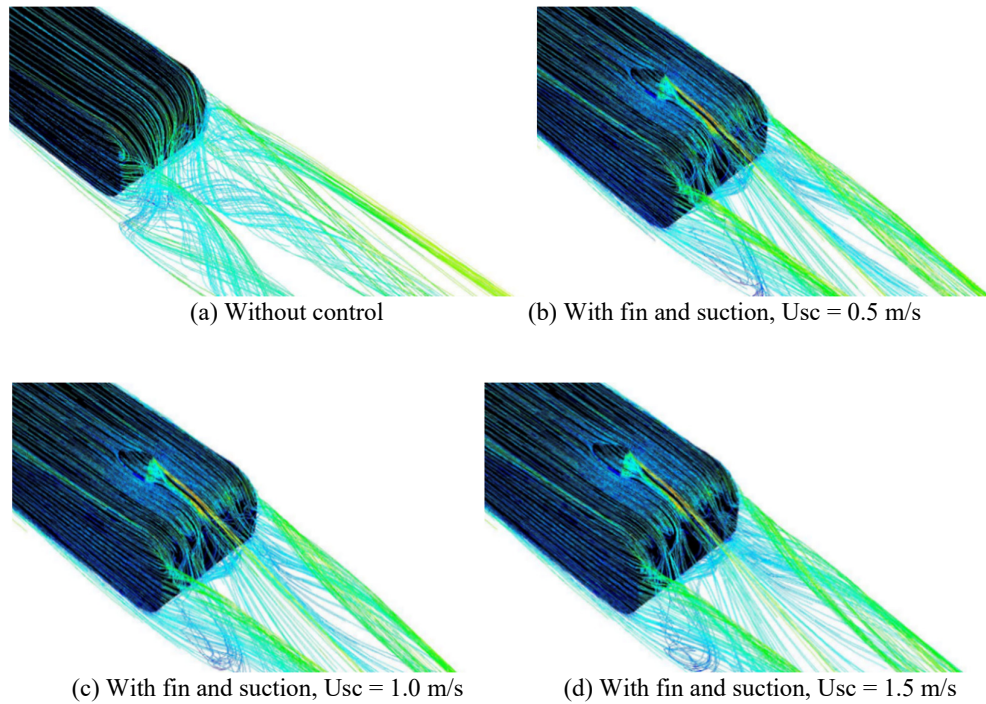


FIGURE 4. Velocity pathline of models with and without fin and suction

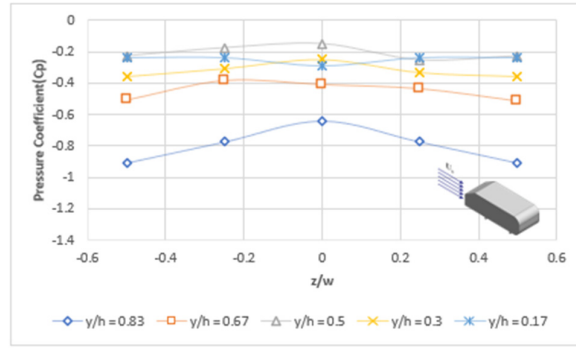
### Pressure Coefficient

The computational results are shown in the following figure. Figure 5 shows the value of the pressure coefficient for the upstream velocity of 22.2 m/s in the absence of rear and upper control. The values of pressure coefficients at the top will show the effect of adding fin before and after. As well as for the pressure coefficient value on the back will show the accumulation of the effect of adding passive fin control and active suction control.

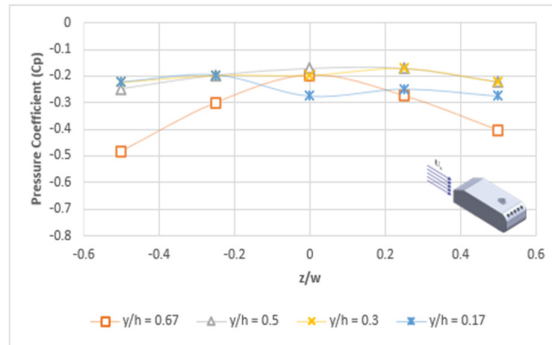
For pressure distribution data on the back of the test model without control and the test model with fins and suction can be seen in table 2.

TABLE 2. The value of the minimum pressure coefficient of the back

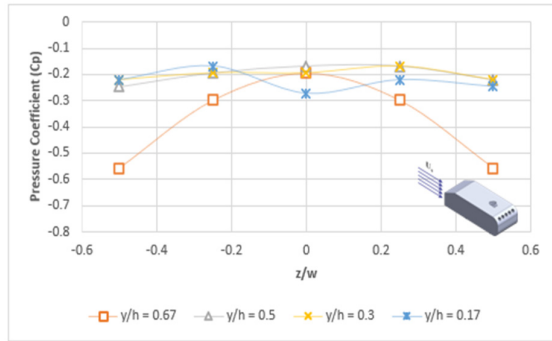
Position (z/w)	Minimum Pressure Coefficient (Cp)			
	Without control	Fin and suction, Usc = 0.5 m/s	Fin and suction, Usc = 1.0 m/s	Fin and suction, Usc = 1.5 m/s
-1/2	-0.909	-0.483	-0.559	-0.672
-1/4	-0.774	-0.300	-0.298	-0.390
0	-0.640	-0.274	-0.275	-0.287
1/4	-0.774	-0.274	-0.298	-0.364
1/2	-0.909	-0.405	-0.559	-0.672



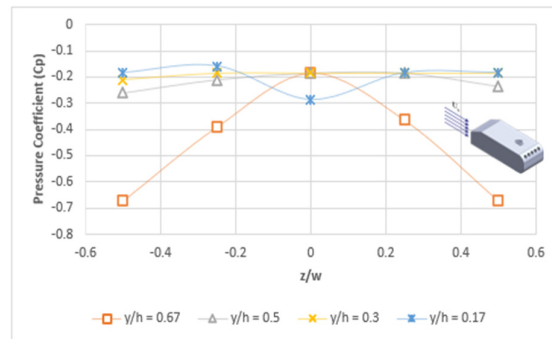
(a) Without control



(b). With fin and suction,  $U_{sc} = 0.5$  m/s



(c). With fin and suction,  $U_{sc} = 1.0$  m/s



(d). With fin and suction,  $U_{sc} = 1.5$  m/s

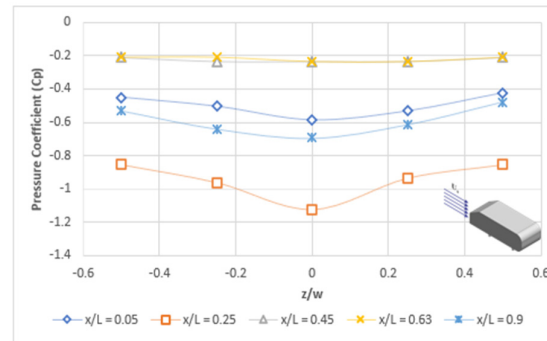
**FIGURE 5.** Pressure distribution on the rear of the test model with and without fin and suction

In Figure 5 a, it is found that the minimum pressure was on the top side of the rear of the model, at the position of the grid size to model height ratio,  $y/h=0.83$ , at position  $z/w=-1/2$  at  $-0.909$ , at position  $z/w=-1/4$  at  $-0.774$ , at position  $z/w=0$  at  $-0.640$ , at position  $z/w=1/4$  at  $-0.774$ , and at position  $z/w=1/2$  at  $-0.909$ . At the position  $y/h=0.83$  the value of  $C_p$  obtained is small, this is due to the fact that it is seen from the flow characteristics at that position that there is a flow separation right on the rear side of the vehicle. In Figure 5 b, the minimum pressure is found on the top side of the rear of the vehicle model, at the position of the grid to model height ratio,  $y/h=0.67$ , at position  $z/w=-1/2$  worth  $-0.483$ , at position  $z/w=-1/4$  is  $-0.300$ , at position  $z/w=0$  is  $-0.274$ , at position  $z/w=1/4$  is  $-0.274$ , and at position  $z/w=1/2$  is  $-0.405$ . In Figure 5 c, it is found that the minimum pressure is on the top side of the rear of the model, at the grid size to model height ratio,  $y/h=0.67$ , at position  $z/w=-1/2$  worth  $-0.559$ , at position  $z/w=-1/4$  is  $-0.298$ , at position  $z/w=0$  is  $-0.271$ , at position  $z/w=1/4$  is  $-0.298$ , and at position  $z/w=1/2$  is  $-0.559$ . In Figure 5 d, it is found that the minimum pressure occurred on the top side of the rear of the model or at the grid size to model height ratio,  $y/h=0.67$ , at position  $z/w=-1/2$  worth  $-0.672$ , at position  $z/w=-1/4$  is  $-0.390$ , at position  $z/w=0$  is  $-0.287$ , at position  $z/w=1/4$  is  $-0.364$ , and at position  $z/w=1/2$  is  $-0.672$ .

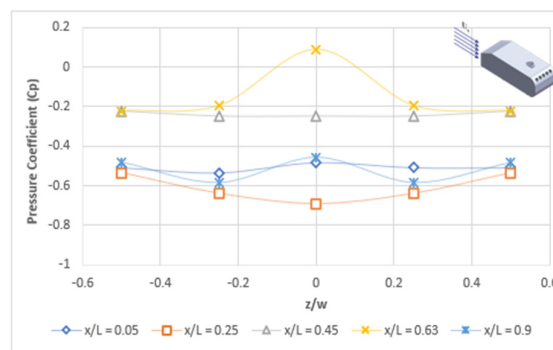
For pressure distribution data at the top of the test model without control and the test model with fins and suction can be seen in table 3.

TABLE 3. The value of the minimum pressure coefficient of the top

Position (z/w)	Minimum Pressure Coefficient ( $C_p$ )	
	Without control	With <i>fin</i> and <i>suction</i>
-1/2	-0.855	-0.534
-1/4	-0.963	-0.638
0	-1.125	-0.690
1/4	-0.936	-0.638
1/2	-0.855	-0.534



(a) Without control



(b) With *fin* and *suction*

FIGURE 6. Pressure distribution on the top of the test model without control and test model with fin and suction

In Figure 6 a, it is found that the minimum pressure occurred on the front area of the top of the model, at the grid size to model length ratio,  $x/L=0.25$ , at position  $z/w=-1/2$  worth  $-0.855$ , at position  $z/w=-1/4$  is worth  $-0.963$ ,

at position  $z/w=0$  is worth -1.125, at position  $z/w=1/4$  is worth -0.936, and at position  $z/w=1/2$  is -0.855. At position  $x/L=0.25$ , the smallest value of  $C_p$  is obtained, this is because flow separation occurs at that position, thus affecting the pressure coefficient value. In figure 6 b, it is found that the minimum pressure occurred on the front area of the top of the model, at the grid size to model length ratio,  $x/L=0.25$ , at position  $z/w=-1/2$  worth -0.534, at position  $z/w=-1/4$  is worth -0.638, at position  $z/w=0$  is -0.690, at position  $z/w=1/4$  is -0.638, and at position  $z/w=1/2$  is -0.534.

### Drag coefficient

Tests carried out to determine the value of the aerodynamic drag coefficient were carried out using a computational approach and an experimental approach. The placement of passive controls in the form of fins and active suction controls on the test model is intended to reduce the amount of aerodynamic drag. To gain a perspective of the effect of the placement of the passive control, a simulation was carried out using the  $C_d$  parameter in Eq. 3, applying the constant density of  $1,225 \text{ kg/m}^3$ , in a frontal area of  $0.0023 \text{ m}^2$ . The data obtained are then displayed in graphs showing comparisons of the aerodynamic drag coefficient ( $C_d$ ) and the suction speed (m/s). The simulated upstream velocity in this study is  $22.2 \text{ m/s}$ . The values of aerodynamic drag of the uncontrolled test model are used as a comparison parameter with the test model using passive controls in the form of fins and active controls in the form of suction. The values of the aerodynamic drag coefficient and the amount of reduction due to the addition of fins and suction both computationally and experimentally are shown in table 3, table 4, and figure 7.

TABLE 3. The values of the computational drag coefficient on the test model with and without fin and suction controls

Drag coefficient ( $C_d$ )				
Upstream speed, $U_0$ (m/s)	Without control	Fin and suction speed (m/s)		
		0.5	1.0	1.5
22.2	1.384	1.150	1.165	1.182
reduction (%)		16.902	15.847	14.647

TABLE 4. The values of the experimental drag coefficient on the test model with and without fin and suction controls

Drag coefficient ( $C_d$ )				
Upstream speed, $U_0$ (m/s)	Without control	Fin and suction speed (m/s)		
		0.5	1.0	1.5
22.2	1.346	1.107	1.121	1.143
reduction (%)		17.757	16.726	15.118

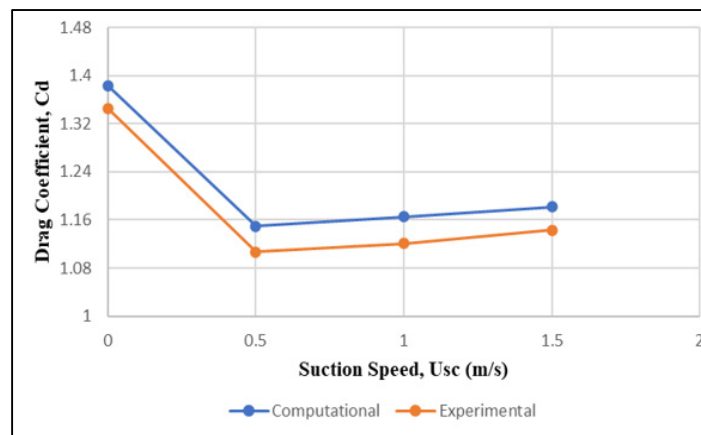


FIGURE 7. Comparison of the drag coefficient values both computationally and experimentally on the test model with and without fin and suction controls.

Based on table 3 and table 4, the largest decrease in drag coefficient value is 16.902% for a suction speed of 0.5 m/s with a drag coefficient value of 1.150 for the computational approach and the largest decrease in drag coefficient value is 17.757% for a suction speed of 0.5 m/s with a value of drag coefficient is 1.107 for the experimental approach. The drag value obtained is in line with the flow characteristics which can be seen in Figure 4, which shows that the most distant flow separation occurs in the application of fin and suction with a speed of  $U_{sc} = 0.5$  m/s and the turbulence formed is smaller than the application of fin and suction. another. The findings are in line with the results of research by Tarakka et al. using an ahmed body with the addition of suction giving the effect of reducing aerodynamic drag by 14.11% [13], and Rumapea et al. with the addition of fins on the ship's rudder reducing the drag value by 64% [10].

## CONCLUSION

1. The addition of passive fin control and active suction control has a positive influence on the characteristics of the flow pattern, where there is a delay in flow separation and the largest reduction in turbulence at the addition of 0.5 m/s suction with an upstream speed of 22 m/s.
2. The addition of passive fin control and active suction control increases the minimum pressure coefficient on the rear wall of the vehicle model. With the highest average minimum pressure coefficient at upstream speed of 22.2 m/s for suction speed of 0.5 m/s of -0.483 with an increase of 56.66% from the model without control -0.801.
3. The addition of passive fin control and active suction control reduces the drag coefficient of the uncontrolled model by 16.902% computationally and by 17.757% experimentally for a suction speed of 0.5 m/s.

## ACKNOWLEDGEMENT

The authors would like to express their gratitude to to the Head and Staff of the Fluid Mechanics Laboratory of the Department of Mechanical Engineering, Faculty of Engineering, Hasanuddin University who have provided facilities in the research.

## REFERENCES

1. S. R. Ahmed, G. Ramm, and G. Faltin, "Some salient features of the time-averaged ground vehicle wake," *SAE Transactions*, pp. 473–503, 1984.
2. R. Tarakka, N. Salam, Jalaluddin, W. Rauf, and M. Ihsan, "Aerodynamic drag reduction on the application of suction flow control on vehicle model with varied upstream velocity," *IOP Conf. Ser.: Mater. Sci. Eng.*, vol. 1173, no. 1, p. 012045, Aug. 2021, doi: 10.1088/1757-899X/1173/1/012045.
3. T. B. Hilleman, "Vehicle drag reduction with air scoop vortex impeller and trailing edge surface texture treatment," US7192077B1, Mar. 20, 2007 Accessed: Nov. 09, 2021. [Online]. Available: <https://patents.google.com/patent/US7192077B1/en>
4. C.-H. Bruneau, E. Creusé, D. Depeyras, P. Gilliéron, and I. Mortazavi, "Coupling active and passive techniques to control the flow past the square back Ahmed body," *Computers and Fluids*, vol. 38, no. 10, p. 1875, 2010, doi: 10.1016/j.compfluid.2010.06.019.
5. T. Ragavan, S. Palanikumar, D. Anastraj, and R. Arulalagan, "Aerodynamic Drag Reduction on Race Cars," *Journal of Basic and Applied Engineering Research*, vol. 1, no. 4, pp. 99–103, 2014.
6. J. Anderson, *Fundamental of Aerodynamics*, 6th ed. Mc Graw Hill, 2017.
7. M. Bellman, R. Agarwal, J. Naber, and L. Chusak, "Reducing Energy Consumption of Ground Vehicles by Active Flow Control," Dec. 2010, pp. 785–793. doi: 10.1115/ES2010-90363.
8. P. Gilliéron, "Detailed analysis of the overtaking process," *Journal of Mechanical Engineering*, no. 54, p. pages-1, 2003.
9. M. Rouméas, P. Gilliéron, and A. Kourta, "Analysis and control of the near-wake flow over a square-back geometry," *Computers & Fluids*, vol. 38, no. 1, pp. 60–70, 2009.
10. M. M. Rumapea, D. Chrismianto, and P. Manik, "The Effect of Adding Fin to the Rudder to Reduce Steering Barriers Using the Cfd Method (Case Study of Kriso Container Ship)," *Jurnal Teknik Perkapalan*, vol. 4, no. 2, 2016.(in Bahasa)
11. Y. N. Putra, P. Manik, and M. Iqbal, "Analysis of the Effect of Variations in Addition of Fin to Centerbulb on MV Catamaran Ship Barriers Laganbar uses the Computational Fluid Dynamic (CFD) method," *Jurnal Teknik Perkapalan*, vol. 5, no. 3, 2017.(in Bahasa)
12. [M. Rouméas, P. Gilliéron, and A. Kourta, "Separated Flows Around the Rear Window of a Simplified Car Geometry," *Journal of Fluids Engineering*, vol. 130, no. 2, Jan. 2008, doi: 10.1115/1.2829566.

13. R. Tarakka, N. Salam, J. Jalaluddin, and M. Ihsan, "Active flow control by suction on vehicle models with variations on front geometry," *International Review of Mechanical Engineering*, vol. 12, no. 2, pp. 128–134, 2018, doi: 10.15866/ireme.v12i2.13876.
14. M. N. Sudin, M. A. Abdullah, S. A. Shamsuddin, F. R. Ramli, and M. Mohd, "Review of Research on Vehicles Aerodynamic Drag Reduction Methods," *International Journal of Mechanical & Mechatronics Engineering IJMME-IJENS*, vol. 14, no. 2, pp. 35–47, 2014.
15. M. Onorato, A. F. Costelli, and A. Garrone, "Drag Measurement Through Wake Analysis," Feb. 1984, p. 840302. doi: 10.4271/840302.
16. H. Harinaldi *et al.*, "Modification of flow structure over a van model by suction flow control to reduce aerodynamics drag," *Makara Journal of Technology*, vol. 16, no. 1, pp. 15–21, 2012.